Cu-based shape memory powder preparation using the mechanical alloying technique

S. Zhang
School of Mechanical and Production Engineering, Nanyang Technological University, Singapore 2263 (Singapore)

L. Lu and M. O. Lai
Department of Mechanical and Production Engineering, National University of Singapore, Singapore 0511 (Singapore)

(Received February 10, 1993; in revised form April 14, 1993)

Abstract

Shape memory powders with nominal compositions of Cu–25.5at.%Zn–5.5at.%Al and Cu–21.1at.%Zn–11.2at.%Al have been prepared starting from commercial powders of Cu84Zn16, Cu70Zn30 and Al using the mechanical alloying (MA) technique. The experimental results show that the microhardness of the mechanically alloyed powders indicates a steady state in which the increase in microhardness due to plastic deformation and the decrease in microhardness due to kinetic annealing have reached a balance. The MA process can still be continued efficiently after the microhardness reaches saturation point. Four stages in the formation of shape memory alloy powder have been identified: the formation of a laminated structure formation, the deformation of the laminated structure, the disappearance of the laminated structure and the formation of alloyed powders. Both X-ray and microstructure data using backscattered electron studies showed that the formation of shape memory powders can be obtained after 7.2 ks milling for 300 rev min^{-1} using a planetary ball mill.

1. Introduction

The mechanical alloying (MA) technique has been used to produce dispersion-strengthened alloys [1–3] and amorphous alloy powders in the solid state [4–6] since the discovery of this technique by Benjamin [7, 8]. One of the advantages of MA is the ease of preparation of alloy powders containing both high and low melting point elements. In this process, powders are cold welded together and then fractured repeatedly during the high energy collision between balls as well as between the balls and the wall of the jar. The repeated welding and fracture finally lead to the formation of alloys or amorphous materials depending on the different elements to be mechanically alloyed. This technique has recently been receiving increasing attention [4]. Different material systems have been investigated.

In the present study, shape memory alloy (SMA) powders for the production of SMAs which are normally prepared by casting and by the powder metallurgy (P/M) method [9] were prepared using the MA technique. In general, it is difficult to obtain homogeneous materials by conventional P/M from element powders because the content of Al powder is very low (about 6 wt.%). A long diffusion time is required to reach homogeneity. Hence pre-alloyed Cu–Zn–Al powder has been exploited for P/M [10, 11]. Normally, three kinds of Cu–Zn–Al pre-alloyed powder with different compositions have to be used to obtain the required composition. In this study, however, only commercial Cu70Zn30, Cu86Zn14 and elemental Al powders were used directly to produce SMA powder with the required composition.

2. Experimental details

Commercial Cu70Zn30 and Cu86Zn14 powders and elemental Al powder were employed to produce SMA powders in the present study. The particle size distributions of these powders are given in Fig. 1. The nominal compositions of the SMA are Cu–25.5at.%Zn–5.5at.%Al and Cu–21.1at.%Zn–11.2at.%Al. The MA process was carried out using a planetary ball mill machine for times varying from 0.9 to 57.6 ks after blending. To reduce oxidation during the milling process, the jar was filled with an argon atmosphere before operation. 16 g of powder were milled each time with 20 stainless steel balls. The ratio of the weight of balls to that of the powders was 20. The speed of the turntable rotation of the planetary ball mill was controlled at 150 and 300 rev min^{-1}. The milled powders were

0921-5093/93/$6.00

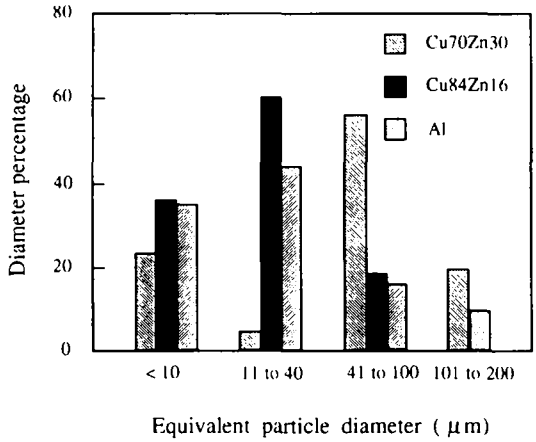

Fig. 1. Particle size distributions of the as-received powders.

characterized by X-ray diffraction analysis with Cu Kα radiation using a Philips PW 1830 X-ray machine operated at 45 kV and 30 mA. The thermal behaviour of the mechanically alloyed powders was analysed at a heating rate and a cooling rate of 10 °C min^{-1} using differential scanning calorimetry (DSC). The distributions of Cu–Zn and Al were analysed on a JEOL JSM-T330A scanning electron microscope operated at 25 kV. The mechanically alloyed powders were cold mounted in resin and then carefully polished. The microhardness of powders was measured using a load of 50 gf and holding for 10 s on an MXT50 microhardness machine.

3. Results and discussion

3.1. Mechanical alloying

MA involves two opposite processes; they are welding between powders and the fracture of powders. In general, at the early stage of milling, welding dominates [12]. At this stage, the powders are easily welded, resulting in an increase in the size of powders. The fracture of powders takes place subsequently. However, the tendency of welding and fracture depends on the properties of the powders to be alloyed. When soft materials are used, welding is excessive while, for brittle materials, fracture dominates. Hence in some cases a processing control agent (PCA) has to be used to prevent excessive welding [13]. It was observed in the present study that the equilibrium between the fracture and welding processes was not naturally achieved when a rotation speed of 300 rev min^{-1} was employed. The reason is that both the Cu–Zn and the Al powders are soft and ductile at room temperature. On high speed milling, the temperature of the powders increased, causing the Cu–Zn and Al powders to become even softer and more ductile so that excessive welding occurred. The size of the powders therefore tended to increase, with relatively larger amounts of the coarser size fraction. The size of the powders was observed to increase to 0.5 mm while the distribution of sizes was not uniform. After MA for 0.9 ks, the powders were even welded to the balls as well as to the inner wall of the jar. The thickness of the welded layer increased with increasing duration of MA. It is, however, of interest to note that, when a ball milling speed of 150 rev min^{-1} was used after MA at 300 rev min^{-1}, not only was the size of the powders reduced to the range 10–45 μm, but also a more uniform powder was gradually formed. Even the powder that was welded onto the balls and the interior wall of the jar was continuously impacted off. The observation therefore indicates that the equilibrium between welding and fracture can be adjusted by controlling the milling speed.

3.2. Microhardness measurement

The microhardness of the milled powders as a function of the MA time is given in Fig. 2. Initially the hardness of the powders increased rapidly because of work hardening. It is observed that the maximum hardness was reached after an MA time of 3.6 ks; then the microhardness decreased until an MA time of 7.2 ks. It is believed that the decrease in microhardness is due to the increase in temperature during MA to enable the hardened powders to be kinetically annealed. After MA for 7.2 ks, the microhardness did not change drastically. It has been suggested that further milling cannot achieve any significant effect on the MA since the powders are fully mechanically alloyed when the saturation point in microhardness is reached [14, 15]. However, in the present study, although the maximum microhardness was reached, it was only a virtual maximum value. It is not a unique measurement to evaluate the degree of MA. Maximum microhardness indicates only that hardening due to plastic deformation and softening due to kinetic annealing have reached a steady state so that no further change could occur. For softer materials, the increase in microhardness can prevent excessive welding and hence the efficiency of MA may be enhanced.

3.3. X-ray diffractometry

Figure 3 illustrates the changes in the X-ray diffraction intensity of Cu–21.1at.%Zn–11.2at.%Al shape memory powder after different MA times. Figure 3, curve (a), shows, as a reference, the X-ray diffraction intensity of the as-received Cu–Zn and Al powders after mixing for 86.4 ks. After MA for 0.9 ks, as shown in Fig. 3, curve (b), only the Al(111) diffraction peak is observed and the intensity of the Al peak has decreased. The Cu70Zn30 and Cu86Zn16 peaks are

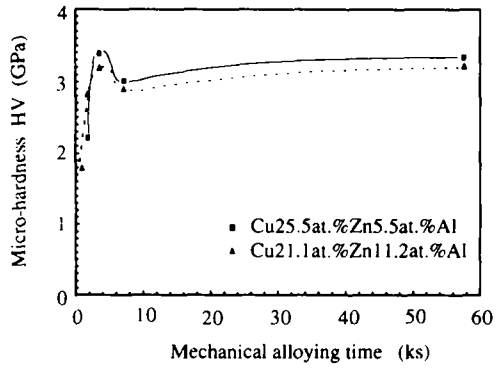

Fig. 2. Vickers' microhardness measurement of mechanically alloyed powders after different milling times.

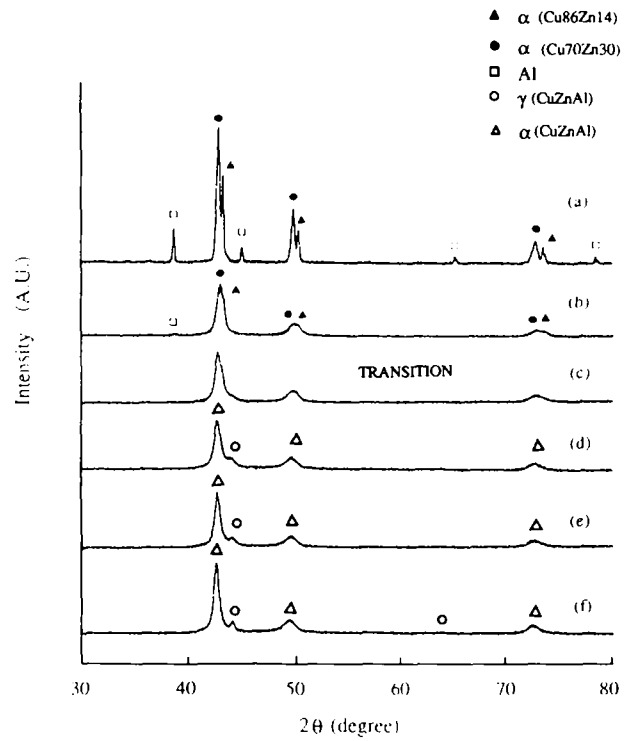

Fig. 3. X-ray intensity of Cu-Zn and Al powders with a composition of Cu-21.1at.%Zn-11.2at.%Al after different milling times (A.u., arbitrary units): curve (a), as received; curve (b), MA for 0.9 ks; curve (c), MA for 1.8 ks; curve (d), MA for 3.6 ks; curve (e) MA for 7.2 ks; curve (f), MA for 57.6 ks.

shifted together, with reductions in the intensities of both peaks. The disappearance of the Al peaks and the shift of the Cu-Zn peaks illustrate the progress of MA. After MA for 1.8 ks, pure elemental Al could no longer be detected, as indicated in Fig. 3, curve (c). Except for the (111) planes of the Cu70Zn30 and Cu86Zn14 powders, the rest of the Cu-Zn peaks were not detectable because of the decrease in intensity. After MA for 3.6 ks, Fig. 3, curve (d), shows no Cu-Zn peak and the α phase of Cu-Zn-Al starts to form on high energy ball milling. On further MA, no significant change in the α phase could be discerned. However, after MA for 3.6 ks, it can be seen in Fig. 3, curve (d), that a peak at $2\theta = 43.90°$ appeared. This peak indicates the formation of the b.c.c. γ phase. The intensity of the peak of (110) plane for the γ phase increased with increase in the MA time (Fig. 3, curve (f)). After MA for 57.6 ks (Fig. 3, curve (f)), another peak of the (200) plane for the γ phase at $2\theta = 63.88°$ was also detectable.

Figure 4, curves (a), (b) and (c), show the changes in X-ray intensity of Cu-25.5at.%Zn-5.5at.%Al powder in the as-received condition, after milling for 3.6 ks and after milling for 57.6 ks respectively. Although no Al element could be observed after milling for 3.6 ks, this does not mean that a fully alloyed powder has been achieved. On comparison with Fig. 3, curve (f), no peaks of the (110) and (200) planes for the γ phase were detected. This is because no γ phase could be produced with a low content of elemental Al. This observation agrees well with the phase diagram produced by Delaey *et al.* [10].

3.4. Microstructure analysis

The distributions of different elements at different milling stages for Cu-2.1at.%Zn-11.2at.%Al are shown in Figs. 5-7. The contrast in the figures corresponds to the atomic number of the laminated structures of Al, Cu70Zn30 and Cu86Zn14 obtained using backscattered electrons. The dark layers show the laminated Al. Figure 5 clearly illustrates the distribution of different elements after MA for 0.9 ks. The laminated layers are thick but their thicknesses are not homogeneous. The thickness of the laminate was observed to decrease with increasing MA time. After MA for 1.8 ks, the discontinuous laminates were found to increase in the grey level as shown in Fig. 6, showing the increase in the degree of MA. After MA for 3.6 ks, as shown in Fig. 7, no laminated structure was observed, indicating the beginning of formation of the Cu-Zn-Al powders. This observation confirms the X-ray result obtained. However, for the composition Cu-25.5at.%Zn-5.5at.%Al, because of the low content of elemental Al, the laminated structure could not be observed after MA for 1.8 ks.

Four stages of MA can be observed in the present study. They are as follows.

(a) *Welding between the powders at the very beginning of MA*. At this stage, the powders are welded together and the welded powders are plastically deformed to a laminated structure.

(b) *Deformation of the laminated structure.* The laminated structure formed is further plastically deformed. The thickness of the laminate continuously decreases until fracture occurs subsequently.

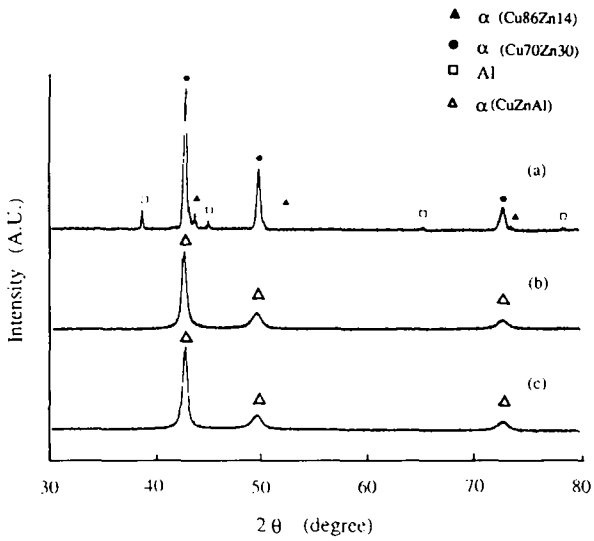

Fig. 4. X-ray intensity of Cu–Zn and Al powders with composition of Cu–25.5at.%Zn–5.5at.%Al after different milling times (A.u., arbitrary units): curve (a), as received; curve (b), MA for 1.8 ks; curve (c), MA for 57.6 ks.

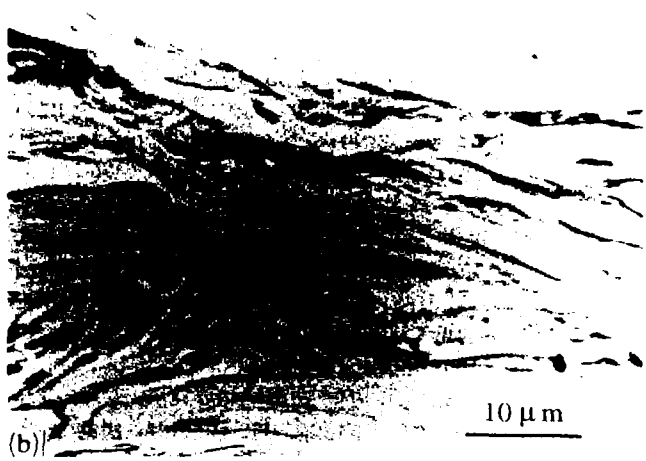

Fig. 5. Typical laminated structure after MA for 0.9 ks.

(c) *Disappearance of the laminated structure.* Here, the laminated structure is fractured and rewelded. As a result, the laminates gradually disappear with increase in the MA.

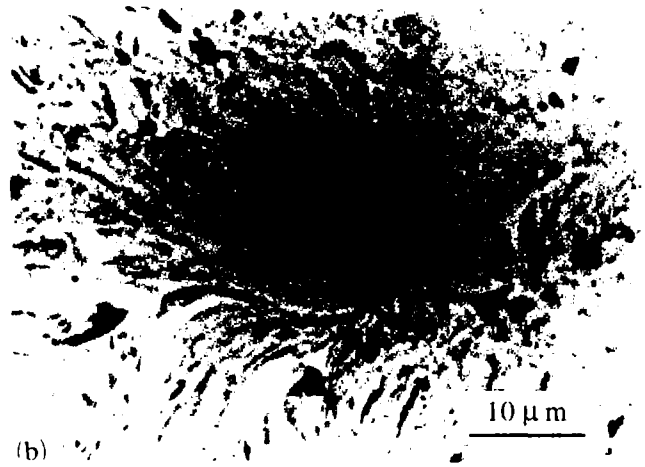

Fig. 6. Typical laminated structure after MA for 1.8 ks.

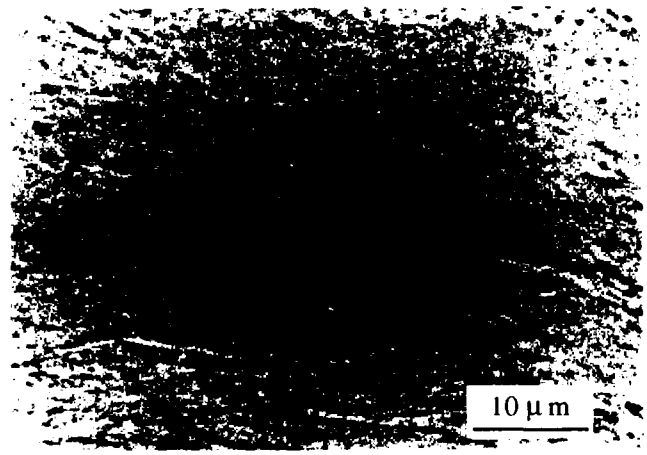

Fig. 7. Typical structure after MA for 3.6 ks. The laminated structure has disappeared.

(d) *Formation of alloy.* At this final stage, alloyed powders are formed through the diffusion mechanism [4]. The increase in defect density induced by heavy plastic deformation and the increase in temperature result in a fast diffusion process.

3.5. Differential scanning calorimetry analysis

Figure 8 shows the DSC results of Cu-21.1at.%Zn-11.2at.%Al SMA powders in the as-milled condition at different times. There is an exothermic heat flow at about 200-250 °C after the powders had been milled for only 0.9 ks. The amount of exothermic heat flow increased when the milling time was increased to 1.8 ks. For longer milling, the heat flow can be seen to decrease. This heat flow also disappears if the powders were thermally rerun a second time. Kinetically, the powders had undergone two simultaneous processes during milling: (1) high energy impact with plastic deformation, leading to an increase in internal energy and hardening; (2) temperature increase, caused by the impact between balls and between the balls and the wall of the jar and by the high speed deformation of powders during milling. This leads to kinetic recovery and partial release of the stored energy. The rest of the stored energy can be released when the powders are thermally cycled. With prolonged milling, the outside surface temperature of the jar was observed to increase from 79 °C, measured after MA for 0.9 ks to about 95 °C measured after MA for 3.6 ks. The temperature at places of impact can be expected to be even higher [16]. Because of the rise in temperature, some of the powders were kinetically recovered during milling. Therefore the amount of exothermic heat flow decreased. The same phenomenon has been observed for the Cu-25.5at.%Zn-5.5at.%Al composition. The change in heat flow as a function of the MA time has been observed to coincide with the change in the microhardness.

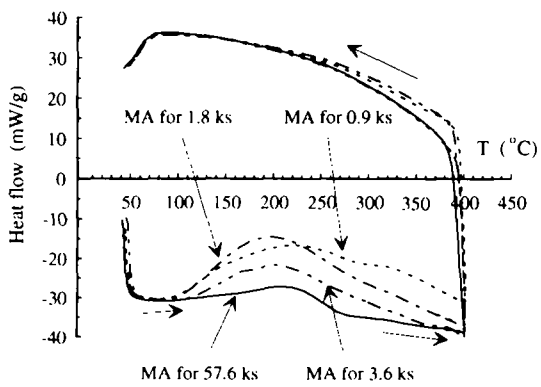

Fig. 8. DSC analysis of Cu-21.1at.%Zn-11.2at.%Al powder after different milling times.

4. Conclusions

(1) Shape memory powders for the production of SMAs can be prepared using the MA method. Four stages have been identified: the formation of a laminated structure, the deformation of the laminated structure, the disappearance of the laminated structure and the formation of alloyed powders.

(2) The measurement of microhardness indicated a steady state point at which the increase in microhardness due to plastic deformation and the decrease in microhardness due to kinetic annealing have reached a balance. For soft materials, it is better to increase the microhardness to prevent excessive welding but, for hard materials, it is better to decrease the microhardness to promote the welding process.

(3) The ball milling speed should be adjusted so that the process of welding between powders and fracture of the welded powders is in equilibrium. At high ball milling speeds, because of the dominating welding process, the distribution of the resulting powder size will not be uniform. It is found that, the higher the ball milling speed, the better is the welding. To obtain a smaller powder size a relatively lower ball milling speed is to be employed.

References

1 G. Jangg, in E. Arzt and L. Schultz (eds.), *New Materials by Mechanical Alloying Techniques*, Informationsgesellschaft, Calw-Hirsau, 1988, p. 39.
2 K. Matsuura and N. Matsuda, in S. Somiya, M. Shimada, M. Yoshimura and R. Watanabe (eds.), *Proc. International Institute for Science of Sintering Symp., Tokyo, November 4-6, 1987*, Elsevier, London, 1987, p. 587.
3 P. Le Brun, X. Niu, L. Froyen, B. Munar and L. Delaey, in A. H. Clauer and J. J. de Barbadillo (eds.), *Solid State Powder Processing*, Minerals, Metals and Materials Society, New York, 1990, p. 273.
4 K. Y. Wang, T. D. Shen, J. T. Wang and M. X. Quan, *Scr. Metall.*, *25* (1991) 2227.
5 Dokyol Lee, J. Cheng, M. Yuan, C. N. J. Wagner and A. J. Ardell, *J. Appl. Phys.*, *64* (9) (1988) 4772.
6 D. Parlapanski, S. Ruseva and E. Gatev, *J. Less-Common Met.*, *171* (2) (1991) 231.
7 J. S. Benjamin, *Metall. Trans.*, *1* (1970) 2943.
8 J. S. Benjamin, in E. Arzt and L. Schultz (eds.), *New Materials by Mechanical Alloying Techniques*, Informationsgesellschaft, Calw-Hirsau, 1988, p. 3.
9 N. Zhang, P. Babayan Khosrovabadi, J. H. Lindenhovius and B. H. Kolster, *J. Phys. (Paris), Colloq. C4*, *1* (1991) 163.
10 L. Delaey, A. Deruyttere, E. Aernoudt and J. R. Roos, Shape memory effect, super-elasticity and damping in copper-zinc-aluminium alloys, *Report 78R1*, February 1, 1978, Department Metaalkunde Katholieke Universiteit Leuven, Belgium.
11 N. Nakanishi and T. Shigematsu, in S. Somiya, M. Shimada, M. Yoshimura and R. Watanabe (eds.), *Proc. of International Institute for Science of Sintering Symp., Tokyo, November 4-6, 1987*, Elsevier, London, 1987, p. 605.

12 J. S. Benjamin and T. E. Volin, *Metall. Trans.*, *5* (1974) 1929.
13 P. S. Gilman and J. S. Benjamin, *Annu. Rev. Mater. Sci.*, *13* (1983) 279.
14 S. Best and W. Bonfield, in J. C. H. Goh and A. Nather (eds.), *Proc. 7th Int. Conf. on Biomedical Engineering, December 2–4, 1992*, BAC Printers, Singapore, 1992, p. 549.
15 P. S. Gilman and W. D. Nix, *Metall. Trans. A*, *12* (1981) 813.
16 P. Le Brun, E. Gaffet, L. Froren and L. Delaey, *Scr. Metall.*, *26* (1992) 1743.